The Riemann Problem for the Simplified Combustion Model in Magnetogasdynamics

Yujin Liu and Wenhua Sun

***Abstract*—The Riemann problem for conservation laws in magnetogasdynamics with combustion is considered. We construct uniquely the Riemann solution with the characteristic analysis method under the modified global entropy conditions and find that the structure of the Riemann solution is similar with that of the conventional gas dynamics combustion model in most cases, while for some cases, there are very different results from each other.**

***Index Terms*—Riemann problem, Characteristic analysis, Hyperbolic conservation laws, Combustion, Magnetogasdynamics.**

I. Introduction

Magnetogasdynamics plays an important role in studying engineering physics and many other aspects ([1], [2], [3], [4], [5], [6], [7], [8], [9], [10]) and is important for the study of the hyperbolic theory. Since the governing equations are highly nonlinear and complicated, the results for Magnetogasdynamics flows are less than the conventional gas dynamics. When the velocity field and the magnetic field are everywhere orthogonal, the magnetogasdynamics flow is simple but still an important model.

In recent years Magnetogasdynamic flows with combustion have attracted much more attention and there are many works done in this aspect([11], [12], [13], [14], [15], [16], [17], [18], etc.). In [13], Helliwell discussed the properties of one-dimensional deflagration waves in a non-conducting inviscid gas at rest when ionization of the gas takes place across a shock wave. The jump relationships across the gas-ionizing shock wave and magnetogasdynamic combustion wave are investigated and the Hugoniot curves are analyzed in the (p, τ) plane. They found that the magnetogasdynamic combustion wave has similar properties to that in conventional gas dynamics.

In [17], Mareev investigated the above results further through the investigation of the one-dimensional self-similar flows caused by piston motion in a hot gas mixture in which a detonation wave or combustion front is propagated. The motion is realized in external electric and magnetic fields which exerts a substantial effect on the flow of the conductive combustion products. The results are used to solve the hypersonic gas flows around a thin wedge in an axial magnetic field.

In the present paper, we are concerned with the one-dimensional inviscid and perfectly conducting compressible fluid with combustion in Lagrangian coordinates

$$\begin{cases} \tau_t - u_x = 0, \\ u_t + (p + \frac{B^2}{2\mu})_x = 0, \\ (E + \frac{B^2\tau}{2\mu})_t + (pu + \frac{B^2 u}{2\mu})_x = 0, \end{cases} \tag{1}$$

with an infinite rate of reaction

$$q(x,t) = \begin{cases} 0, & \text{if } \sup\limits_{0\le y\le t} T(x,y) > T_i; \\ q(x,0), & \text{otherwise}, \end{cases} \tag{2}$$

under the assumption $B = k\rho$, where $\tau > 0$, $p \ge 0$, u, $B \ge 0$ and μ are the specific volume, pressure, velocity, transverse magnetic field and magnetic permeability, respectively. $E = e + \frac{u^2}{2} + q$ is the specific total energy, where e is the specific internal energy and q is the chemical binding energy. The temperature T satisfies Boyle and Gay-Lussac's law: $p\tau = RT$. T_i is the ignition temperature. For polytropic gases, we know $e = e(T)$ and $E = \frac{u^2}{2} + \frac{p\tau}{\gamma-1} + q$, where $\gamma > 1$ is the adiabatic exponent. For simplicity, we usually assume that R and γ remain unchanged during the reaction. We also assume that the combustion process is exothermic, i.e., the energy used up in recombing the atoms to form the new molecules is smaller for the burnt gas than the binding energy of the unburnt gas [21].

Although the governing equations of magnetogasdynamics are more complex than the conventional gas dynamics equations, many results of the one-dimensional magnetogasdynamics flow are similar with the conventional gas dynamics. However the contact discontinuity is very different from each other. Unlike the conventional gas dynamics, where the image of the contact discontinuity in the space (τ, p, u) is a straight line parallel to the τ-axis and the projection on the plane (p, u) is a point, the contact discontinuity is a plane curve in the space (τ, p, u) and the projection on the plane (p, u) is a straight line parallel to the p-axis which causes that the Riemann solutions are more complicated and difficult than that of the conventional gas dynamics.

In [4], Hu and Sheng obtained constructively the unique solution of the Riemann problem for (1) with the characteristic analysis method. Notice that the results are of the non-combustion case for one-dimensional magnetogasdynamics flow (1).

In the present study, we construct the Riemann solutions of the Chapman-Jouguet (CJ) model (1) and (2) with the following initial data

$$(\tau, p, u, q)(x, 0) = (\tau^\pm, p^\pm, u^\pm, q^\pm), \quad \pm x > 0, \tag{3}$$

where $\tau^\pm > 0, p^\pm, u^\pm$ are arbitrary constants,

$$q^\pm = \begin{cases} 0, & \text{if } T^\pm > T_i, \\ 0 \text{ or } q_0, & \text{if } T^\pm \le T_i, \end{cases}$$

This work is supported by the Foundation for Young Scholars of Shandong University of Technology (No. 115024).

Yujin Liu is with School of Mathematics and Statistics, Shandong University of Technology, Zibo, Shandong, 255000, P. R. China.

Wenhua Sun is with School of Mathematics and Statistics, Shandong University of Technology, Zibo, Shandong, 255000, P. R. China. Yujin Liu is the corresponding author. (e-mail: yjliu98@126.com (Y.J. Liu))

(Advance online publication: 20 November 2019)

and $q_0 > 0$ is a constant.

The Riemann problem of the conventional gas dynamics combustion models and the other related problems in partial differential equations were investigated by many researchers ([19], [20], [21], [22], [23], [24], [25], [26], [27], [28], [29], etc.). Zhang and Zheng [29] studied the Riemann problem of the one-dimensional adiabatic, inviscid flow of combustible ideal gases with an infinite rate of reaction which is described by

$$\begin{cases} u_t + p_x = 0, \\ \tau_t - u_x = 0, \\ E_t + (up)_x = 0, \\ q(x,t) = \begin{cases} 0, & \text{if } \sup\limits_{0\le y\le t} T(x,y) > T_i; \\ q(x,0), & \text{otherwise.} \end{cases} \end{cases} \tag{4}$$

In order to guarantee the uniqueness of the solution, they proposed a set of entropy conditions containing the point-wise and the global entropy conditions. Under the entropy conditions, they constructed the Riemann solutions with the characteristic analysis method and discussed the wave interactions of the shock wave with the combustion waves.

In [23], we modified the global entropy conditions in [29] and constructed the unique solution of the generalized Riemann problem for (4) under the modified entropy conditions with the characteristic method.

In this paper, we construct uniquely the Riemann solutions of (1), (2) with the initial data (3) under the modified entropy conditions in [23]. We find that the structures of the Riemann solutions are similar with that of the conventional gas dynamic combustion model (4) in most cases. However, for some cases, our results are very different from (4). For example, for Case 2. in Section 3, there exists a possible deflagration wave solution for (1) and (2) while there is no deflagration wave solution but a possible detonation wave solution of the corresponding case in the conventional gas dynamics combustion model in [23] and [29].

The rest of this paper is arranged as follows. In Section II, we present some preliminaries and study the properties of the elementary combustion waves. In Section III, we investigate the Riemann problem of the model (1), (2) with the initial values (3) under the modified global entropy conditions. A final conclusion is given in Section IV.

II. Preliminaries and elementary combustion wave

In this section, we study the elementary wave curves and give some important properties of the elementary wave curves for our later discussions.

A. Noncombustion wave curves in the (τ, p) or (u, p) plane

First, we investigate the non-combustion elementary wave curves for (1). For details we refer readers to [4].

There are three eigenvalues of (1) which are $\lambda_- = -(\frac{p - e_p\frac{BB_\tau}{\mu} + e_\tau}{e_p})^{\frac{1}{2}}$, $\lambda_0 = 0$ and $\lambda_+ = (\frac{p - e_p\frac{BB_\tau}{\mu} + e_\tau}{e_p})^{\frac{1}{2}}$. If $e_p > 0$ and $e_\tau + p > 0$, they are real and distinct, thus (2) is a strictly hyperbolic system. It is easily shown that the characteristic fields $\lambda_\pm$ are genuinely nonlinear and the characteristic field λ_0 is linearly degenerate.

Looking for the self-similar solution $(\tau, p, u)(\xi)(\xi = \frac{x}{t})$, we know that for any smooth solution it holds that

$$\begin{cases} \xi \mathrm{d}\tau = -\mathrm{d}u, \\ \xi \mathrm{d}u = \mathrm{d}(p + \frac{B^2 u}{2\mu}), \\ \xi \mathrm{d}(E + \frac{B^2 u}{2\mu}\tau) = \mathrm{d}(up + \frac{B^2 u}{2\mu}u). \end{cases} \tag{5}$$

For the polytropic gas, the forward or backward rarefaction waves in the (τ, p, u) space passing through the point $Q_0(\tau_0, p_0, u_0)$ are given by

$$\overleftrightarrow{R}: \begin{cases} p\tau^\gamma = p_0\tau_0^\gamma, \\ u = u_0 \pm \int_{p_0}^{p} \frac{\sqrt{\gamma p\tau + \frac{B^2\tau}{\mu}}}{\gamma p}\mathrm{d}p. \end{cases} \tag{6}$$

The Rankine-Hugoniot jump conditions at $\xi = \sigma$ are

$$\begin{cases} \sigma[\tau] = -[u], \\ \sigma[u] = [p + \frac{B^2 u}{2\mu}], \\ \sigma[E + \frac{B^2 u}{2\mu}\tau] = [up + \frac{B^2 u}{2\mu}u], \end{cases} \tag{7}$$

where $[\tau] = \tau_r - \tau_l$, etc.

The contact discontinuity can be expressed as

$$J: \quad [u] = [p + \frac{B^2}{2\mu}] = \sigma = 0, \tag{8}$$

and it is easy to see that J is a curve with $u = Const.$ in the (τ, p, u) space and the projection on the (p, u) plane is a straight line parallel to the p-axis. Denote the contact discontinuity J by $\overset{<}{J}$ when $p_l < p_r,\ \tau_l < \tau_r$, and $\overset{>}{J}$ when $p_l > p_r,\ \tau_l > \tau_r$.

If $[q] = 0$ in (7), we get the forward or backward shock waves in the (τ, p, u) space passing through the point $Q_0(\tau_0, p_0, u_0)$

$$\begin{cases} (p + \theta^2 p_0 + \theta^2(\frac{3B^2}{2\mu} + \frac{B_0^2}{2\mu}))\tau = (p_0 + \theta^2 p \\ +\theta^2(\frac{3B_0^2}{2\mu} + \frac{B^2}{2\mu}))\tau_0, \\ u = u_0 \pm (p + \frac{B^2}{2\mu} - p_0 - \frac{B_0^2}{2\mu})(-\frac{\tau - \tau_0}{p + \frac{B^2}{2\mu} - p_0 - \frac{B_0^2}{2\mu}})^{\frac{1}{2}}, \end{cases} \tag{9}$$

where $\theta^2 = \frac{\gamma-1}{\gamma+1}$ and $B_0 = \frac{k}{\tau_0}$. The properties of R, J and S can be found in [4].

For convenience and conciseness, we denote the projection of $\overleftrightarrow{R}(\overleftrightarrow{S})$ on the (τ, p) plane and (u, p) plane by $R_u(S_u)$ and $\overleftrightarrow{R}_\tau(\overleftrightarrow{S}_\tau)$, respectively.

B. Combustion wave curves in the (τ, p) plane

Here we discuss the combustion wave curves in the (τ, p) plane.

If $[q] \neq 0$ in (7), from the explicit expression (9) of the shock wave curve in the (τ, p) plane, fixing the value on the front side of the discontinuity to (τ_0, p_0, q_0) while allowing $(\tau, p, 0)$ on the back side vary, we obtain that

$$\begin{aligned} &\tfrac{p\tau}{\gamma-1} + \tfrac{B^2\tau}{2\mu} - \tfrac{p_0\tau_0}{\gamma-1} - q_0 - \tfrac{B_0^2\tau_0}{2\mu} \\ &+\tfrac{1}{2}(p_0 + \tfrac{B_0^2}{2\mu} + p - \tfrac{B^2}{2\mu})(\tau - \tau_0) = 0, \end{aligned} \tag{10}$$

and by a direct computation it follows that

$$D_u(0): \quad (\tau-\theta^2\tau_0)(p+\theta^2(p_0+\frac{B_0^2}{2\mu}+\frac{3B^2}{2\mu}))$$
$$=(1-\theta^4)\tau_0 p_0+\frac{\theta^2\tau_0}{\mu}[B_0^2(3-\theta^2)+B^2(1-3\theta^2)]$$
$$+2\theta^2 q_0. \tag{11}$$

$D_u(0)$ is called the combustion wave curve in the (τ, p) plane.

Lemma 2.1 The combustion wave curve $D_u(0)$ is convex and monotonically decreasing. Furthermore, it is a branch of a hyperbola with $\tau=\theta^2\tau_0$ and $p=-\theta^2(p_0+\frac{B_0^2}{2\mu})$ as its asymptotes ($\tau>\theta^2\tau_0$, $p>-\theta^2(p_0+\frac{B_0^2}{2\mu})$) and the state (τ_0, p_0) is located below this curve.

Proof. Differentiating along the curve $D_u(0)$ with respect to τ, it yields that

$$\frac{\mathrm{d}p}{\mathrm{d}\tau}=\frac{-p-\theta^2 p_0-\frac{\theta^2 k^2}{2\mu}\frac{(\tau-\tau_0)(\tau^2+\tau\tau_0-2\tau_0^2)}{\tau^3\tau_0^2}}{\tau-\theta^2\tau_0}<0,$$

thus $D_u(0)$ is monotonically decreasing.

For the convexity, in the same way with the proof of Lemma 3.4. in [4], we know that $\frac{\mathrm{d}^2 p}{\mathrm{d}\tau^2}>0$ and $D_u(0)$ is convex. ■

Draw two straight lines from the point (τ_0, p_0) which are tangent to the curve. Similar with that of the conventional gas dynamics combustion model ([29]), we call the tangent points C with $\tau<\tau_0$ and D with $\tau>\tau_0$ Chapman-Jouguet detonation ($CJDT$) and Chapman-Jouguet deflagration (CJDF), respectively. From the RH condition (7), we have $\sigma=\pm\sqrt{-\frac{[p+\frac{B^2}{2\mu}]}{[\tau]}}$ and it follows that we should disregard the curve between the points A and B where $(p+\frac{B^2}{2\mu}-p_0-\frac{B_0^2}{2\mu})(\tau-\tau_0)>0$. We call the curve between A and C weak detonation (WDT) and the curve above C strong detonation (SDT), the curve between B and D weak deflagration (WDF) and the curve below D strong deflagration (SDF), respectively (see Fig. 2.1.).

From the known Jouguet's rule ([29]), we know that there are at most three different kinds of wave series that can be linked to the state $(-)\equiv(\tau_-, p_-, u_-, q_-)$:

(i) $S_u(-)$ or $R_u(-)$ (containing no combustion waves),

(ii) $(i)+WDF(i)$ or $(i)+CJDF(i)+R(CJDF(i))$ (containing no DT waves),

(iii) $SDT(-)$ or $CJDT(-)+R(CJDT(-))$ (containing no DF waves),

where $i\equiv i(-)\equiv(u_i, p_i, \tau_i, q)$ is the state at $S(-)$ with the ignition temperature T_i, and the symbol +" means followed by". Notice that we let the temperature behind the shock wave which is the known pre-compressive shock wave connecting the state $(-)$ and the ignition point (i) be the ignition point T_i, thus we just need to construct the deflagration wave curve which is the successor to the pre-compressive shock wave from the point (i).

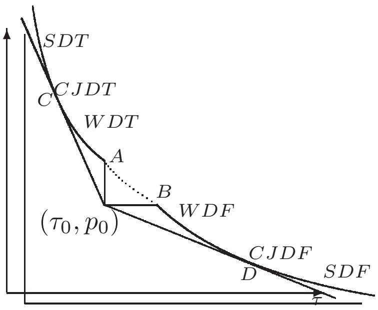

Fig. 2.1. The combustion wave curve in the (τ, p).

In the (τ, p)-plane we have the following expressions:

$$R_u(-): p\tau^\gamma=p_-\tau_-^\gamma, \quad (0<p<p_-),$$
$$S_u(-): (\tau-\theta^2\tau_-)(p+\theta^2(p_-+\frac{B_-^2}{2\mu}+\frac{3B^2}{2\mu}))$$
$$=(1-\theta^4)\tau_- p_-+\frac{\theta^2\tau_-}{\mu}[B_-^2(3-\theta^2)+B^2(1-3\theta^2)],$$
$$(p>p_-),$$
$$SDT(-): (\tau-\theta^2\tau_-)(p+\theta^2(p_-+\frac{B_-^2}{2\mu}+\frac{3B^2}{2\mu}))$$
$$=(1-\theta^4)\tau_- p_-+\frac{\theta^2\tau_-}{\mu}[B_-^2(3-\theta^2)+B^2(1-3\theta^2)]$$
$$+2\theta^2 q_0, \quad (p>p_C),$$
$$WDF(i): (\tau-\theta^2\tau_i)(p+\theta^2(p_i+\frac{B_i^2}{2\mu}+\frac{3B^2}{2\mu}))$$
$$=(1-\theta^4)\tau_i p_i+\frac{\theta^2\tau_i}{\mu}[B_i^2(3-\theta^2)+B^2(1-3\theta^2)]$$
$$+2\theta^2 q_0, \quad ((p_D)_i<p<p_i),$$
$$R(CJDT(-)): p\tau^\gamma=p_C\tau_C^\gamma, \quad (p<p_C),$$
$$R(CJDF(-)): p\tau^\gamma=(p_D)_i(\tau_D)_i^\gamma, \quad (p<(p_D)_i). \tag{12}$$

Denote $W(-):=W_S(-)\cup W_D(-)$, where $W_S(-)$ denotes $(W_S(-), \; q_-=0)$ or $(W_S(-), \; q_->0)$ or both of them, and $W_D(-)$ denotes $W_{DT}(-)\cup W_{DF}(-)$, here $W_{DT}(-):=SDT(-)\cup CJDT(-)\cup R(CJDT(-))$ and $W_{DF}(-):=WDF(i)\cup CJDF(i)\cup R(CJDT(i))$.

Lemma 2.2 The combustion wave curve $W_{DF}(-)$ in the (τ, p) plane is located above both the segment $\overline{(-)(i)}$ and the rarefaction wave curve $R_u(-)$.

Proof. The proof is similar with Lemma 1. in [29] and here we omit it for simplicity. ■

C. Combustion wave curves in the (u, p) *plane*

We investigate the explicit expressions and the important properties of the combustion wave curves in the (u, p) plane. We construct the backward combustion wave curve $\overleftarrow{W}(-)$ from the state $(-)=(\tau_-, p_-, u_-, q_-)$.

If $q_-=0$, the backward wave curve is

$$\overleftarrow{W}_S(-):=\overleftarrow{S}_\tau(-)\cup\overleftarrow{R}_\tau(-),$$

which is the noncombustion wave curve from the state $(-)$ (see Fig. 2.2. left). From Lemma 3.5. and Lemma 3.6. in [4], $\overleftarrow{S}_\tau(-)$ and $\overleftarrow{R}_\tau(-)$ are convex and monotonically decreasing.

If $q_->0$, the backward wave curve is composed of three branches: one is the backward noncombustion wave curve

$(\overleftarrow{W}_S(-), q_- > 0)$ (see Fig. 2.2. right) which is the same as $\overleftarrow{W}_\tau(-), q_- = 0$ except that along the curve it holds that $q_- > 0$ and its top end is the ignition point (u_i, p_i), where

$$u_i = u_- - \sqrt{(p_i + \frac{B_i^2}{2\mu} - p_- - \frac{B_-^2}{2\mu})(\tau_- - \tau_i)},$$

from now on $\overleftarrow{W}_S(-)$ denotes $(\overleftarrow{W}_S(-), q_- > 0)$ or $(\overleftarrow{W}_S(-), q_- = 0)$ or both of them; the other two are the combustion DF and DT wave curves. Next we discuss the combustion wave curves in the (u, p) plane.

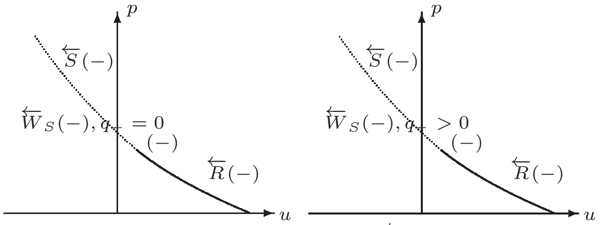

Fig. 2.2. The backward noncombustion wave curve $\overleftarrow{W}_S(-)$ in the (u, p) plane.

From the explicit expressions (9), for the backward wave $\overleftarrow{S}_\tau(Q_{0\tau})$ we get

$$u = u_0 - \sqrt{(p + \frac{B^2}{2\mu} - p_0 - \frac{B_0^2}{2\mu})(\tau_0 - \tau)}, \quad u < u_0,$$

on the other hand, we know that

$$\tau = \frac{(1-\theta^4)\tau_0 p_0 + \frac{\theta^2\tau_0}{\mu}[B_0^2(3-\theta^2) + B^2(1-3\theta^2)] + 2\theta^2 q_0}{p + \theta^2(p_0 + \frac{B_0^2}{2\mu} + \frac{3B^2}{2\mu})} + \theta^2\tau_0, \tag{13}$$

and

$$\tau - \tau_0 = \frac{(1-\theta^2)\tau_0(p_0 - p) + \frac{\theta^2\tau_0}{\mu}(B_0^2 - B^2) + 2\theta^2 q_0}{p + \theta^2(p_0 + \frac{B_0^2}{2\mu} + \frac{3B^2}{2\mu})},$$

thus we obtain the backward combustion wave curve $\overleftarrow{D}_\tau(0)$ in the (u, p) plane

$$u = u_0 - \sqrt{\frac{\mu(p)}{p + \theta^2(p_0 + \frac{B_0^2}{2\mu} + \frac{3B^2}{2\mu})}}, \tag{14}$$

where

$$\mu(p) = (p + \frac{B^2}{2\mu} - p_0 - \frac{B_0^2}{2\mu})[(1-\theta^2)\tau_0(p - p_0) + \frac{\theta^2\tau_0}{\mu}(B^2 - B_0^2) - 2\theta^2 q_0]. \tag{15}$$

Lemma 2.3 The combustion wave curve $\overleftarrow{D}_\tau(0)$ is convex and monotonically decreasing.

Proof. Since

$$-\frac{u - u_0}{p - p_0} = -\sqrt{\frac{\tau - \tau_0}{p + \frac{B^2}{2\mu} - p_0 - \frac{B_0^2}{2\mu}}}, \tag{16}$$

it follows that $\frac{\tau_0 - \tau}{p + \frac{B^2}{2\mu} - p_0 - \frac{B_0^2}{2\mu}} > 0$, we know

$$p + \frac{B^2}{2\mu} > p_0 + \frac{B_0^2}{2\mu}, \quad \tau < \tau_0,$$

or

$$p + \frac{B^2}{2\mu} < p_0 + \frac{B_0^2}{2\mu}, \quad \tau > \tau_0.$$

From (9) we obtain

$$(u - u_0)^2 = (p + \frac{B^2}{2\mu} - p_0 - \frac{B_0^2}{2\mu})(\tau_0 - \tau).$$

Differentiating along the curve with respect to p, it yields that

$$2(u - u_0)\frac{du}{dp} = (p + \frac{B^2}{2\mu} - p_0 - \frac{B_0^2}{2\mu})(-\frac{d\tau}{dp}) + (\tau_0 - \tau)(1 - \frac{k^2}{\mu}\frac{1}{\tau^3})\frac{d\tau}{dp}. \tag{17}$$

From Lemma 2.1., $\frac{dp}{d\tau} < 0$, it turns out that $\frac{du}{dp} < 0$, thus $\overleftarrow{D}_\tau(0)$ is monotonically decreasing curve.

For the convexity, in the same way with the proof of Lemma 3.5. in [4], it yields that $\frac{d^2u}{dp^2} > 0$ and $\overleftarrow{D}_\tau(0)$ is convex. ■

Theorem 2.1 The combustion wave curve $\overleftarrow{D}_\tau(0)$ loses meaning when $0 < p - p_0 < \frac{\gamma-1}{\tau_0}q_0$, and $u = u_0$ when $p = p_0$ or $p = p_0 + \frac{\gamma-1}{\tau_0}q_0$. Moreover, $u \to +\infty$ when $p \to -\theta^2(p_0 + \frac{B_0^2}{2\mu})$ and $u \to -\infty$ when $p \to +\infty$.

Theorem 2.2 In the (τ, p) plane, along the curve $D_u(0)$ we know that $\frac{p-p_0}{\tau-\tau_0}$ has its maximum and minimum at $CJDT$ and $CJDF$ point, respectively. It follows that the counterpart in the (u, p) plane $\frac{p-p_0}{u-u_0}$ has respectively its maximum and minimum at $\overleftarrow{CJDT}$ and $\overleftarrow{CJDF}$ point due to (16). Furthermore, each of the two curves is monotonic along SDT(or $\overleftarrow{SDT}$), WDT (or $\overleftarrow{WDT}$), WDF(or $\overleftarrow{WDF}$), SDF(or $\overleftarrow{SDF}$), respectively.

We depict the backward combustion wave curve $\overleftarrow{D}_\tau(0)$ as in Fig. 2.3. Now denote the backward DF and DT wave curve by $\overleftarrow{W}_{DF}(-)$ and $\overleftarrow{W}_{DT}(-)$, respectively, where

$$\overleftarrow{W}_{DF}(-) := \overleftarrow{WDF}(i_s) \cup \overleftarrow{CJDF}(i_s) \cup \overleftarrow{R}(\overleftarrow{CJDF}(i_s)),$$
$$\overleftarrow{W}_{DT}(-) := \overleftarrow{SDT}(-) \cup \overleftarrow{CJDT}(-) \cup \overleftarrow{R}(\overleftarrow{CJDT}(-)).$$

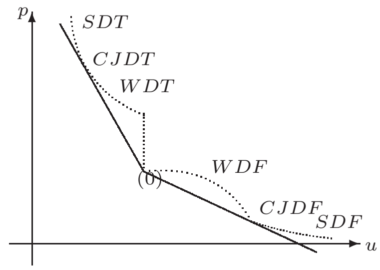

Fig. 2.3. The backward combustion wave curve in the (u, p) plane.

Since the combustion wave curves are exactly similar with that of the conventional gas dynamics, we obtain similar results of the properties for the combustion wave curves $\overleftarrow{W}_{DF}(-)$ and $\overleftarrow{W}_{DT}(-)$ with Lemma 2. in [29] in the same way. Here we just list the results.

Lemma 2.4 The combustion wave curves $\overleftarrow{W}_{DF}(-)$ and $\overleftarrow{W}_{DT}(-)$ in the (u, p) plane are located above the noncombustion wave solution $\overleftarrow{W}_S(-)$.

Denote the backward wave curve $\overleftarrow{W}(-)$ (see Fig. 2.4.) which can be linked to the state $(-) = (\tau_-, p_-, u_-, q_-)$, then

$$\overleftarrow{W}(-) := \overleftarrow{W}_S(-) \cup \overleftarrow{W}_D(-),$$

$$\overleftarrow{W}_S(-) := (\overleftarrow{W}_S(-), q^- = 0) \ or \ (\overleftarrow{W}_S(-), q^- > 0),$$

$$\overleftarrow{W}_D(-) := \overleftarrow{W}_{DF}(-) \cup \overleftarrow{W}_{DT}(-).$$

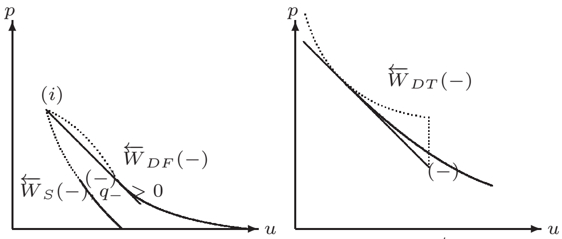

Fig. 2.4. The backward combustion wave curve $\overleftarrow{W}(-)$.

Similarly, we can construct the forward combustion wave curve $\overrightarrow{W}(+)$ which can be linked to the state $(+) = (\tau_+, p_+, u_+, q_+)$.

III. Solutions of the Riemann problem (1) and (2) with the initial data (3)

We shall study the Riemann problem of the CJ model (1) and (2) with the initial values (3). When $q_- = q_+ = 0$ which means the gas on both sides are burnt, no combustion wave will occur. For this case, the Riemann solutions have been constructed in [4], for simplicity we omit them.

When q_- and q_+ are not both zero, there may exist more than one intersection points of $\overleftarrow{W}(-)$ and $\overrightarrow{W}(+)$. Each intersection point corresponds to a unique Riemann solution. When the intersection point is unique, the solution is also unique, otherwise, in order to obtain the unique solution we select it under the following *modified global entropy conditions (MGEC) ([23]):*

we select the unique solution from the nine intersection points (at most) of the forward wave curves connecting $(+)$ and the backward wave curves connecting $(-)$ in the following order:

A. the solution with the propagating speed of combustion wave as low as possible;

B. the solution with the parameter β as small as possible, where β is defined as oscillation frequency of $T(\xi)$ between the set $\{\xi \in R^1 : T(\xi) \leq T_i\}$ and the set $\{\xi \in R^1 : T(\xi) > T_i\}$;

C. the solution containing as many combustion wave as possible.

For simplicity, we just consider the Riemann problem (1), (2) and (3) in the following three cases. For the other cases, we can obtain the results similarly.

Case 1. $q^- > 0,\ q^+ = 0$. In this case, the gas is unburnt on the left side, the gas is burnt on the right side, i.e., $\overleftarrow{W}(-) = \overleftarrow{W}_S(-) \cup \overleftarrow{W}_{DF}(-) \cup \overleftarrow{W}_{DT}(-)$, $\overrightarrow{W}(+) = \overrightarrow{W}_S(+)$. When there exists only one intersection point of $\overleftarrow{W}(-)$ and $\overrightarrow{W}(+)$, we obtain the unique solution is a detonation wave solution $\overleftarrow{DT} + \overrightarrow{R} \ or \ \overrightarrow{S}$ if $p_-\tau_-^\gamma = p_+\tau_+^\gamma$, or $\overleftarrow{DT} + J + \overrightarrow{R} \ or \ \overrightarrow{S}$ if $p_-\tau_-^\gamma \neq p_+\tau_+^\gamma$ based on the arguments in [4]. In what follows we suppose that there are three intersection points of $\overleftarrow{W}(+)$ and $\overrightarrow{W}_S(+)$. We only present the case in Fig. 3.1.

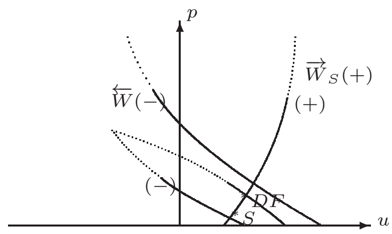

Fig. 3.1. $q^- > 0,\ q^+ = 0$ and there are three interaction points.

From Lemma 2.2. and Lemma 2.6., we know the propagating speed of the deflagration wave is less than that of the detonation wave. Therefore due to the global entropy condition *A* the intersection point of $\overrightarrow{W}_S(+)$ and $\overleftarrow{W}_{DT}(-)$ should be discarded. We denote the intersection point of $\overrightarrow{W}_S(+)$ and $\overleftarrow{W}_S(-)$ by $*_S$ and the intersection point of $\overrightarrow{W}_S(+)$ and $\overleftarrow{W}_{DF}(-)$ by $*_{DF}$. We denote the temperature at the point $*_S$, $*_{DF}$ on $\overrightarrow{W}_S(+)$ by T_S, T_{DF}, respectively. The temperature at $*_{DF}$ on $\overleftarrow{W}_{DF}(-)$ is greater than T_i according to the assumption that the combustion process is exothermic (Fig. 3.2).

Subcase 1.1. $p_-\tau_-^\gamma = p_+\tau_+^\gamma$.

We select the point $*_S$ or $*_{DF}$ and obtain the possible solution is $\overleftarrow{R} \ or \ \overleftarrow{S} + \overrightarrow{R} \ or \ \overrightarrow{S}$ or $\overleftarrow{DF} + \overrightarrow{R} \ or \ \overrightarrow{S}$. Now we construct the unique Riemann solution under the modified global entropy conditions as follows.

a) When $T^+ > T_i$, then $\beta(*_S) = 1$, $\beta(*_{DF}) = 1$, from the condition *C*, we select $*_{DF}$ and obtain a combustion wave solution $\overleftarrow{DF} + \overrightarrow{R} \ or \ \overrightarrow{S}$ (Fig. 3.2. (ii)).

b) When $T^+ \leq T_i$, then $\beta(*_S) = 0$, $\beta(*_{DF}) = 2$, from the condition *B*, we select $*_S$ and obtain a noncombustion wave solution $\overleftarrow{R} \ or \ \overleftarrow{S} + \overrightarrow{R} \ or \ \overrightarrow{S}$ (Fig. 3.2. (i)).

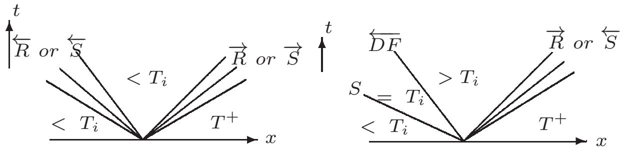

(i) noncombustion wave (ii) combustion wave *DF*

Fig. 3.2. Solutions in Subcase 1.1.

Subcase 1.2. $p_-\tau_-^\gamma \neq p_+\tau_+^\gamma$.

From the condition *A*, we discard the possible detonation DT wave solution and find that the possible Riemann solution is $\overleftarrow{R} \ or \ \overleftarrow{S} + J + \overrightarrow{R} \ or \ \overrightarrow{S}$ or $\overleftarrow{DF} + J + \overrightarrow{R} \ or \ \overrightarrow{S}$. According to the modified global entropy conditions we obtain the unique Riemann solution as follows (Fig. 3.3.).

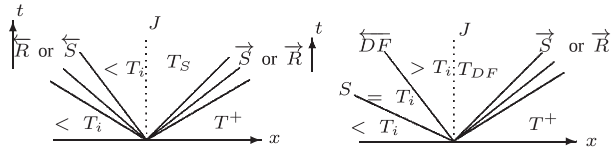

(i) noncombustion wave (ii) combustion wave *DF*

Fig. 3.3. Solutions in Subcase 1.2.

a) When $T^+ > T_i$, $T_{DF} > T_i$, then $\beta(*_S) = 1$, $\beta(*_{DF}) = 1$, from the condition *C*, we select $*_{DF}$ and obtain a combustion wave solution containing a DF (Fig. 3.3. (ii)).

b) When $T^+ > T_i$, $T_{DF} \leq T_i (\Rightarrow T_S \leq T_i)$, then $\beta(*_S) = 1$, $\beta(*_{DF}) = 3$, from the condition *B*, we select $*_S$ and obtain a noncombustion wave solution (Fig. 3.3. (i)).

c) When $T^+ \le T_i,\ T_S \le T_i$, then $\beta(*_S) = 0$, $\beta(*_{DF}) = 2$, from the condition *B*, we select $*_S$ and obtain a noncombustion wave solution (Fig. 3.3. (i)).

d) When $T^+ \le T_i, T_S > T_i (\Rightarrow T_{DF} > T_i)$, then $\beta(*_S) = 2$, $\beta(*_{DF}) = 2$, from the condition *C*, we select $*_{DF}$ and obtain a combustion wave solution containing a DF (Fig. 3.3. (ii)).

Case 2. $q^- > 0,\ q^+ = 0$ and there are two intersection points of $\overleftarrow{W}(+)$ and $\overrightarrow{W}_S(+)$.

Just as the above case, we denote the intersection point of $\overrightarrow{W}_S(+)$ and $\overleftarrow{W}_{DT}(-)$ by $*_{DT}$ and the temperature at the point $*_{DT}$ on $\overrightarrow{W}_S(+)$ by T_{DT} (Fig. 3.4).

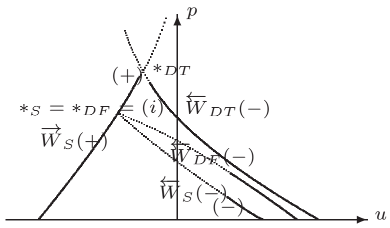

Fig. 3.4. $q^- > 0,\ q^+ = 0$ and there are two intersection points.

Subcase 2.1. $p_-\tau_-^\gamma = p_+\tau_+^\gamma$.

In this case, we select the point $*_S$ or $*_{DT}$ and obtain the possible solutions $\overleftarrow{S} + \overrightarrow{R}\ or\ \overrightarrow{S}$ or $\overleftarrow{DT} + \overrightarrow{R}\ or\ \overrightarrow{S}$. Now we select the unique Riemann solution as follows.

a) When $T^+ > T_i$, then $\beta(*_S) = 1$, $\beta(*_{DT}) = 1$, from the condition *C*, we select $*_{DT}$ and obtain a combustion wave solution $\overleftarrow{DT} + \overrightarrow{R}\ or\ \overrightarrow{S}$ (Fig. 3.5. (i)).

b) When $T^+ \le T_i$, then $\beta(*_S) = 0$, $\beta(*_{DT}) = 2$, from the condition *B*, we select $*_S$ and obtain a noncombustion wave solution $\overleftarrow{S} + \overrightarrow{R}\ or\ \overrightarrow{S}$ (Fig. 3.5. (ii)).

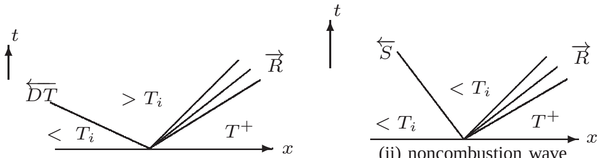

(i) combustion wave *DT* (ii) noncombustion wave

Fig. 3.5. Solutions in Subcase 2.1.

Subcase 2.2. $p_-\tau_-^\gamma \ne p_+\tau_+^\gamma$.

In this case, we know that there are two possibilities: one is that there exists only one intersection point of $\overleftarrow{W}(-)$ and $\overrightarrow{W}(+)$ and we obtain the unique Riemann solution is $\overleftarrow{DT} + \overset{>}{J} + \overrightarrow{R}\ or\ \overrightarrow{S}$, the other one is that there are three possible solutions which are the noncombution wave solution $\overleftarrow{S}\ or\ \overleftarrow{R} + J + \overrightarrow{R}\ or\ \overrightarrow{S}$, or the DF combustion wave solution $\overleftarrow{DF} + J + \overrightarrow{R}\ or\ \overrightarrow{S}$, or the DT combustion wave solution $\overleftarrow{DT} + \overset{<}{J} + \overrightarrow{R}\ or\ \overrightarrow{S}$. Similarly, according to the modified global entropy conditions we obtain the unique solution as follows (Fig. 3.6.). From the global entropy condition *A*, we discard the DT combustion wave solution.

a) When $T^+ > T_i$, $T_{DF} > T_i$, then $\beta(*_S) = 1$, $\beta(*_{DF}) = 1$, from the condition *C*, we select $*_{DF}$ and obtain a combustion wave solution containing a DF (Fig. 3.6. (ii)).

b) When $T^+ > T_i, T_{DF} \le T_i (\Rightarrow T_S \le T_i)$, then $\beta(*_S) = 1$, $\beta(*_{DF}) = 3$, from the condition *B*, we select $*_S$ and obtain a noncombustion wave solution (Fig. 3.6. (i)).

c) When $T^+ \le T_i,\ T_S \le T_i$, then $\beta(*_S) = 0$, $\beta(*_{DF}) = 2$, from the condition *B*, we select $*_S$ and obtain a noncombustion wave solution (Fig. 3.6. (i)).

d) When $T^+ \le T_i, T_S > T_i (\Rightarrow T_{DF} > T_i)$, then $\beta(*_S) = 2$, $\beta(*_{DF}) = 2$, from the condition *C*, we select $*_{DF}$ and obtain a combustion wave solution containing a DF (Fig. 3.6. (ii)).

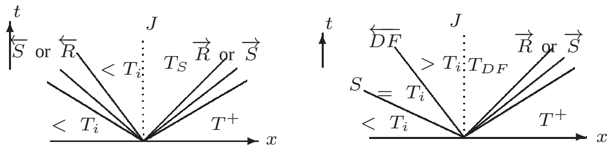

(i) noncombustion wave (ii) combustion wave *DF*

Fig. 3.6. Solutions in Subcase 2.2.

Theorem 3.1 In this case, for the combustion model (1) and (2) in magnetogasdynamics, there exists a possible deflagration wave solution for our Riemann problem which is different from the conventional gas dynamics in [23] and [29] where there is no deflagration wave solution but only a possible detonation wave solution of the corresponding case.

Case 3. $q^- > 0,\ q^+ > 0$ and the gas on the both sides are unburnt. In this case ,we know that $\overleftarrow{W}(-) = \overleftarrow{W}_S(-) \cup \overleftarrow{W}_{DF}(-) \cup \overleftarrow{W}_{DT}(-)$, $\overrightarrow{W}(+) = \overrightarrow{W}_S(+) \cup \overrightarrow{W}_{DF}(+) \cup \overrightarrow{W}_{DT}(+)$.

If the intersection point of $\overleftarrow{W}(-)$ and $\overrightarrow{W}(+)$ is unique, the solution is a detonation wave solution $\overleftarrow{DT} + \overrightarrow{DT}$ if $p_-\tau_-^\gamma = p_+\tau_+^\gamma$, or $\overleftarrow{DT} + J + \overrightarrow{DT}$ if $p_-\tau_-^\gamma \ne p_+\tau_+^\gamma$ based again on the results in [4]. Otherwise, there are two possible subcases: one is that there is an intersection point of $\overleftarrow{W}_S(-)$ and $\overrightarrow{W}_S(+)$, the other is that there is no intersection point of $\overleftarrow{W}_S(-)$ and $\overrightarrow{W}_S(+)$.

Case 3.1. In the former subcase (Fig. 3.7.), we discuss it in the following two subcases.

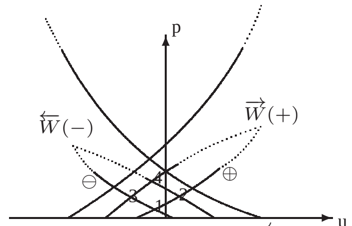

Fig. 3.7. There is an intersection point of $\overleftarrow{W}_S(-)$ and $\overrightarrow{W}_S(+)$.

Subcase 3.1.1. $p_-\tau_-^\gamma = p_+\tau_+^\gamma$.

From the condition *A*, we just need to consider the intersection points 1, 2, 3, 4. We should select the unique solution from the four possible solutions (Fig. 3.8.).

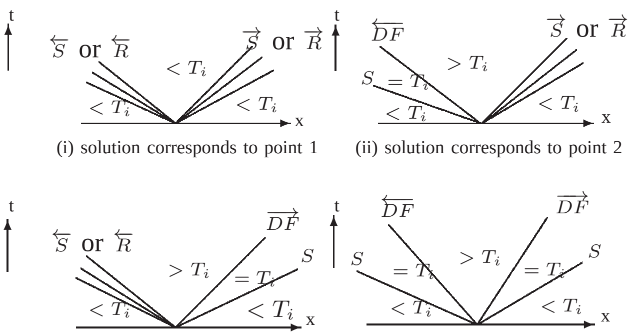

(i) solution corresponds to point 1 (ii) solution corresponds to point 2

(iii) solution corresponds to point 3 (iv) solution corresponds to point 4

Fig. 3.8. The possible solutions in Subcase 3.1.1.

It is obvious that $\beta = 0$ for (i), and it holds that $\beta = 2$ for (ii), (iii) and (iv). From the condition *B*, we select the intersection point 1 and obtain the unique noncombustion wave solution $\overleftarrow{R}\ or\ \overleftarrow{S} + \overrightarrow{R}\ or\ \overrightarrow{S}$.

Subcase 3.1.2. $p_-\tau_-^\gamma \neq p_+\tau_+^\gamma$. In a similar way as the above discussions in Subcase 3.1.1., we obtain that the unique Riemann solution is still the noncombustion wave solution $\overleftarrow{R}\ or\ \overleftarrow{S} + J + \overrightarrow{R}\ or\ \overrightarrow{S}$. The only difference is that here the contact discontinuity appears.

Case 3.2. In the latter subcase, there are only two possibilities: $\overleftarrow{W}(-)$ intersects $\overrightarrow{W}_{DT}(+)$ only or $\overrightarrow{W}(+)$ intersects $\overleftarrow{W}_{DT}(-)$ only. We just need to consider the former. If the intersection point is unique, the solution is $\overleftarrow{DT} + \overrightarrow{DT}$ if $p_-\tau_-^\gamma = p_+\tau_+^\gamma$, or $\overleftarrow{DT}+J+\overrightarrow{DT}$ if $p_-\tau_-^\gamma \neq p_+\tau_+^\gamma$, otherwise, there are at most three intersection points (Fig. 3.9.).

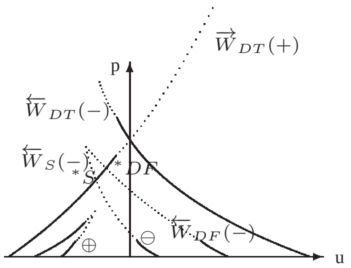

Fig. 3.9. $\overleftarrow{W}(-)$ intersects $\overrightarrow{W}_{DT}(+)$ only.

Subcase 3.2.1. $p_-\tau_-^\gamma \neq p_+\tau_+^\gamma$.

In this subcase (Fig. 3.10.), from the condition *A*, the intersection point of $\overleftarrow{W}_{DT}(-)$ and $\overrightarrow{W}_{DT}(+)$ should be discarded. We denote the intersection point of $\overrightarrow{W}_{DT}(+)$ and $\overleftarrow{W}_S(-)$ by $^*S$ and denote the intersection point of $\overrightarrow{W}_{DT}(+)$ and $\overleftarrow{W}_{DF}(-)$ by $^*DF$, respectively. We denote the temperature at the point $^*S$, $^*DF$ on $\overrightarrow{W}_{DT}(+)$ by T_S, T_{DF}, respectively.

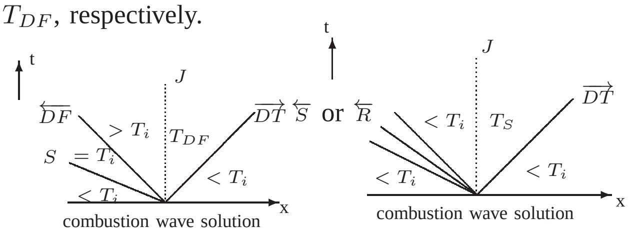

Fig. 3.10. Solutions in Subcase 3.2.1.

Since $T_S > T_i$ we have $T_{DF} > T_i$, then $\beta(^*S) = 2$, $\beta(^*DF) = 2$. From the condition *C*, we select $^*DF$ and obtain a combustion wave solution $\overleftarrow{DF} + \overrightarrow{DT}$.

Subcase 3.2.2. $p_-\tau_-^\gamma = p_+\tau_+^\gamma$. In a similar way as the above discussions in Subcase 3.2.1., we obtain that the unique Riemann solution is still the combustion wave solution $\overleftarrow{DF} + \overrightarrow{DT}$. The only difference is that there exists the contact discontinuity in Subcase 3.2.1..

IV. Conclusion

In this work, we find that there exists a unique piecewise smooth solution of the Riemann problem (1) (2) with the initial data (3) under the modified global entropy conditions (MGEC).

Since the reaction rate in our model is infinite which is an idealized hypothesis, while our model is still very important in application, we will investigate the initial value problem for the self-similar Zeldovich-von Neumann-Döring (ZND) model in magnetogasdynamic combustion with finite reaction rate in our coming works.

Publication Ethics Statement

The authors declare that there are no conflicts of interest regarding the publication of this paper.

References

[1] H. Cabannes, "Theoretical magnetofluid dynamics, Academic Press(Applid Mathematics and Mechanics Series," vol. 13, New York, 1970.

[2] G.Q. Chen, D.H. Wang, "Global Solutions of Nonlinear Magnetohydrodynamics with Large Initial Data," *Journal of Differential Equations*, vol. 182, No. 2, pp. 344-376, 2002.

[3] T.G. Cowling, "Magnetoydrodynamics," *Interscience*, New York, 1957.

[4] Y.B. Hu, W.C. Sheng, "The Riemann problem of conservation laws in magnetogasdynamics," *Communications on Pure and Applied Analysis*, vol. 12, No. 2, pp. 755-769, 2013.

[5] D.Q. Li, T.H. Qin, "Physics and partial differential equations," *Higher Education Press* (Chinese Series), 2005.

[6] X.K. Pu, B.L. Guo, "Global existence and convergence rates of smooth solutions for the full compressible MHD equations," *Zeitschrift fr angewandte Mathematik und Physik*, vol. 64, No. 3, pp. 519-538, 2013.

[7] T.R. Sekhar, V.D. Sharma, "Riemann problem and elementary wave interactions in isentropic magnetogasdynamics," *Nonlinear Analysis: Real World Applications*, vol. 11, No. 2, pp. 619-636, 2010.

[8] C. Shen, "The limits of Riemann solutions to the isentropic magnetogasdynamics," *Applied Mathematics Letters*, vol. 24, No.7, pp. 1124-1129, 2011.

[9] Q.F. Wu, H. Li, "Magnetogasdynamics," *National Defense Science and Technology University Press* (Chinese Series), 2007.

[10] Y.F. Yang, X.H. Gu, C.S. Dou, "Existence and uniqueness of steady solutions to the magnetohydrodynamic equations of compressible flows," *Journal of Mathematical Analysis and Applications*, vol. 409, No. 2, pp. 846-850, 2014.

[11] A.A. Barmin, L.N. Lebedeva, "Structure of ionizing detonation waves in the presence of an electromagnetic field," *Fluid Dynamics*, vol. 10, No.6, pp. 952-959, 1975.

[12] A.R. Gordon, J.B. Helliwell, "Magnetogasdynamic deflagration under the Chapman-Jouguet condition," *Journal of Fluid Mechanics*, vol. 23, No. 4, pp. 779-786, 1965.

[13] J.B. Helliwell, "Gas-ionizing shock and combustion waves in magnetogasdynamics," *Journal of Fluid Mechanics*, vol. 14, No. 3, pp. 405-419, 1962.

[14] J.B. Helliwell, "Magnetogasdynamic deflagration and detonation waves with ionization," *Journal of Fluid Mechanics*, vol. 16, No. 2, pp. 243-261, 1963.

[15] J.B. Helliwell, "Magnetogasdynamic effects on the growth of transverse acoustic waves in a reacting gas," *Zeitschrift fur Angewandte Mathematik und Physik*, vol. 34, pp. 406-411, 1983.

[16] F.G. Liu, "Life-span of classical solutions for one-dimensional hydromagnetic flow," *Applied Mathematics and Mechanics* (English Edition), vol. 28, No. 4, pp. 511-520, 2007.

[17] V.A. Mareev, "Self-similar magnetogasdynamic flows accompanied by detonation and combustion waves," *Fluid Dynamics*, vol. 10, No. 1, pp. 86-93, 1975.

[18] L.P. Singh, A. Husain, M. Singh, "On the evolution of weak discontinuities in radiative magnetogasdynamics," *Acta Astronautica*, vol. 68, No. 1-2, pp. 16-21, 2011.

[19] S.A. Altaie, A.F. Jameel, A. Saaban, "Homotopy Perturbation Method Approximate Analytical Solution of Fuzzy Partial Differential Equation," *IAENG International Journal of Applied Mathematics*, vol. 49, No. 1, pp. 22-28, 2019.

[20] J.B. Bacani, and G. Peichl, "The Second-Order Eulerian Derivative of a Shape Functional of a Free Boundary Problem," *IAENG International Journal of Applied Mathematics*, vol. 46, No. 4, 425-436. 2016.

[21] R. Courant, K.O. Friedrichs, "Supersonic Flow and Shock Waves," Interscience, New York, 1948.

[22] J.Q. Li, P. Zhang, "The transition from Zeldovich-von Neumann-Döring to Chapman-Jouguet theories for a nonconvex scalar combustion model," *SIAM Journal on Mathematical Analysis*, vol. 34, No. 3, pp. 675-699, 2003.

[23] Y.J. Liu, W.C. Sheng, "The generalized Riemann problem for gas dynamic combustion," *Applied Mathematics and Mechanics* (English Edition), vol. 32, No. 8, pp. 1079-1090, 2011.

[24] W.C. Sheng, M.N. Sun, T. Zhang, "The generalized Riemann problem for a scalar nonconvex Chapman-Jouguet combustion model," *SIAM Journal on Applied Mathematics*, vol. 68, No. 2, pp. 544-561, 2007.

[25] M.N. Sun, "Entropy Solutions of a Chapman-Jouguet Combustion model," *Mathematical Models and Methods in Applied Sciences*, vol. 22, No. 9, pp. 1250018 (35 pages), 2012.

[26] Z.H. Teng, A.J. Chorin, T. P. Liu, "Riemann problems for reacting gas with application to transition," *SIAM Journal on Applied Mathematics*, vol. 42, No. 5, pp. 964-981, 1982.

[27] F.A. Williams, "Combustion Theory," *Benjamin Commings*, Menlo Park, 1985.

[28] J.Q. Xie, D.W. Deng and H.S. Zheng, "A Compact Difference Scheme for One-dimensional Nonlinear Delay Reaction-diffusion Equations with Variable Coefficient," *IAENG International Journal of Applied Mathematics*, vol. 47, No. 1, pp. 14-19, 2017.

[29] T. Zhang, Y.X. Zheng, "Riemann problem for gasdynamic combustion," *Journal of Differential Equations*, vol. 77, No. 2, pp. 203-230, 1989.